JOURNAL OF AIRCRAFT
Vol. 31, No. 4, July–Aug. 1994

Doublet-Point Method for Supersonic Unsteady Aerodynamics of Nonplanar Lifting-Surfaces

Ashish Tewari*
Indian Institute of Technology, Kanpur 208016, India

A new method is devised for the calculation of pressures and aerodynamic influence-coefficients on nonplanar lifting-surface configurations oscillating in a supersonic freestream. The method is an extension of the methodology introduced in the planar supersonic doublet-point scheme, which is based upon the concept of concentrated lift forces and uses the acceleration potential doublet as an elementary solution of the wave equation. These features make the method capable of being incorporated in a unified code for both subsonic and supersonic speeds, as well as amenable to rapid aeroelastic calculations. Results on various lifting-surface configurations are in agreement with other supersonic oscillatory methods, validating the doublet-point approximation in nonplanar supersonic applications.

Introduction

FOR studying the aeroelastic characteristics and aeroservoelastic interactions of modern supersonic aircraft, an efficient method of predicting the unsteady supersonic aerodynamics of practical lifting configurations is required. The unsteady aerodynamic loads due to a general motion of the structure can be derived from those arising out of simple harmonic motion, by using analytic continuation in the Laplace domain. Hence, an oscillatory supersonic lifting-surface theory becomes necessary. The supersonic counterpart of the subsonic doublet-lattice method,[1] which is well established for its amenability to aeroelastic calculations, has been sought in the past[2] without much success. Nevertheless, motivation for a supersonic scheme with enough commonality with the subsonic doublet-lattice method to have a unified code for both the speed regimes, has persisted.

Garrick and Rubinow[3] presented an integral equation for the supersonic velocity potential source-strength. The most common velocity potential solution procedure is the Mach box method introduced by Pines et al.,[4] and further refined by several authors.[5–9] Difficulties with the Mach box method include the necessity to evaluate velocity potential in diaphragm regions off the lifting surface and the dependence of the grid on Mach number. The refinements suggested to alleviate these difficulties add complexity to the method. Another velocity potential approach is the extension of Evvard's[10] steady-state theory to the oscillatory case by Burkhart.[11] This scheme eliminates the need for diaphragm regions, but is limited to planar applications.

Jones and Appa[12] proposed the potential-gradient method. They used a series expansion of the kernel function, which made the scheme less accurate at high frequencies. Hounjet[13] avoided the series expansion by using an integration scheme similar to that of the subsonic doublet-lattice method[1] for directly downstream receiving points. Chen and Liu[14] applied another approach to avoid the series expansion by using a parabolic curve-fit for the exponential part of the integrand, in order to integrate the dipole spanwise singularity of the planar kernel. The schemes of Refs. 12–14 needed to consider the wake region between lifting surfaces. Also, the computation of pressure influence-coefficients required additional steps in these schemes since they did not formulate a direct relationship between pressure and normalwash. Appa[15] rederived the potential-gradient integral equation and arrived at a direct relationship between pressure and normalwash. Reference 15 also showed that the kernel could be expressed in a form analytic on the Mach cone, and evaluated the nonplanar interference by using a finite difference approximation. There was no need to integrate on the wake region lying between the lifting surfaces. The recently published Harmonic-Gradient ZONA51C scheme of Liu et al.[16] uses the same integral formulation as Appa.[15] Reference 16 claims to handle all kernel integrations analytically, but an absence of details prevents meaningful discussion. It is also implied in Ref. 16 that the method uses a doublet-lattice type curve-fit approximation (cf. Ref. 14), which appears to contradict the claim of exact integrations.

The third category of supersonic lifting-surface methods adopts the acceleration potential doublet as the elementary solution of the wave equation. The advantage of this approach lies in using the same integral equation as that for subsonic flow. This integral equation can also be obtained by using a rederived potential-gradient formulation.[15,16] Watkins and Berman[17] derived the integral equation from the acceleration potential approach. Harder and Rodden[18] provided the nonplanar kernel function for the integral equation. One solution procedure is the kernel function method of Cunningham,[19] which uses assumed pressure polynomials whose coefficients are determined by satisfying the normalwash boundary condition at a number of collocation points. Lottati and Nissim[20] developed a variation of this approach by employing box-like divisions with a continuous pressure polynomial in each box. The supersonic kernel function methods[19,20] are extremely sensitive to the choice of pressure polynomials. Ueda and Dowell[21] proposed another type of acceleration potential scheme, called the supersonic doublet-point method, limited to planar applications. It uses concentrated lift forces (or point doublets) and an averaged normalwash for discretizing the integral equation. The most attractive feature of this scheme is that it affords the greatest degree of similarity between subsonic and supersonic calculations. Ueda and Dowell[22] had earlier devised a subsonic doublet-point method using the same concept of discrete acceleration potential doublets and distributed normalwash. Questions arose[23,24] about the validity of the doublet point approximation, since it reversed the traditional discretization procedure. However, Ueda and Dowell[21,22] demonstrated the concept's validity for planar cases in both subsonic and supersonic calculations. The subsonic

Received Jan. 31, 1993; revision received April 5, 1993; presented as Paper 93-1588 at the AIAA 34th Structures, Structural Dynamics, and Materials Conference, La Jolla, CA, April 19–21, 1993; accepted for publication June 14, 1993.

*Assistant Professor, Aerospace Engineering. Member AIAA.

and supersonic doublet-point methods can be combined into one code since they differ only in the kernel integration. This, and the concentrated lift-force assumption of the doublet-point scheme, are invaluable features when repeated aeroelastic calculations are to be carried out efficiently. Tewari[25,26] extended the supersonic doublet point method to nonplanar applications. When compared to the planar kernel function, the nonplanar kernel is of a very complicated character, with strong Mach cone singularities. The normalwash averaging procedure has to account for Mach boundary curvature in nonplanar interference, leading to many more averaging cases than a planar configuration. As a consequence, the general nonplanar supersonic doublet-point method is a much more complex undertaking than the planar scheme of Ueda and Dowell.[21]

Integral Equation

The integral equation relating pressure difference amplitude ΔC_p across the lifting surface at point (X, Y, Z), and the normalwash amplitude w at a point (ξ, η, ζ) on a nonplanar lifting configuration placed in a uniform supersonic freestream of velocity U and oscillating at a frequency ω, is[25,26]

$$w(\xi, \eta, \zeta) = \frac{1}{8\pi} \int \int_W \Delta C_p(X, Y, Z) \times K(\xi - X, \eta - Y, \zeta - Z, \omega)\, dX\, dY \tag{1}$$

The integration in Eq. (1) is performed over that area W of the lifting-surface which is contained within the upstream Mach cone emanating from the normalwash point (Fig. 1). The kernel function in Eq. (1) can be expressed as

$$K(x, y, z, k) = K_1(x, y, z, k)T_1 + K_2(x, y, z, k)T_2 \tag{2}$$

where

$$T_1 = \cos(\gamma_r - \gamma_s)$$

$$T_2 = (Z_0 \cos \gamma_r - Y_0 \sin \gamma_r)(Z_0 \cos \gamma_s - Y_0 \sin \gamma_s)$$

$$Z_0 = z \cos \gamma_s + \sin \gamma_s, \quad Y_0 = y \cos \gamma_s - \sin \gamma_s$$

$$K_1(x, y, z, k) = \frac{M^2 e^{-ikx}}{R}\left(\frac{e^{-ikX_1}}{x + X_1} + \frac{e^{-ikX_2}}{x + X_2}\right) + e^{-ikx}\int_{X_1}^{X_2} \frac{e^{-ikv}\, dv}{(r^2 + v^2)^{3/2}} \tag{3}$$

$$K_2(x, y, z, k) = \frac{e^{-ikx}}{r^4}\left[\frac{\beta^2 M^2 r^4}{R^3}\left(\frac{e^{-ikX_1}}{x + X_1} + \frac{e^{-ikX_2}}{x + X_2}\right) - \frac{ikM^3 r^4}{R^2}\left(\frac{e^{-ikX_1}}{x + X_1} - \frac{e^{-ikX_2}}{x + X_2}\right) - \frac{M^5 r^4}{R^2}\left(\frac{X_1 e^{-ikX_1}}{(x + X_1)^3} - \frac{X_2 e^{-ikX_2}}{(x + X_2)^3}\right) - \frac{2M^4 r^4}{R}\left(\frac{e^{-ikX_1}}{(x + X_1)^3} + \frac{e^{-ikX_2}}{(x + X_2)^3}\right) - 3r^4 \int_{X_1}^{X_2} \frac{e^{-ikv}}{(r^2 + v^2)^{5/2}}\, dv\right] \tag{4}$$

$$X_1 = (x - MR)/\beta^2, \quad X_2 = (x + MR)/\beta^2$$

$$x = (\xi - X)/b, \quad y = (\eta - Y)/b, \quad z = (\zeta - Z)/b$$

$$R = \sqrt{x^2 - \beta^2 r^2}, \quad r = \sqrt{y^2 + z^2}$$

$$\beta = \sqrt{M^2 - 1}, \quad M = U/a$$

$k = \omega b/U$ is the nondimensional reduced frequency, b is a reference length, and γ_s and γ_r are the dihedral angles at the sending (pressure) and receiving (normalwash) points, (X, Y, Z) and (ξ, η, ζ), respectively, and a is the speed of sound far upstream.

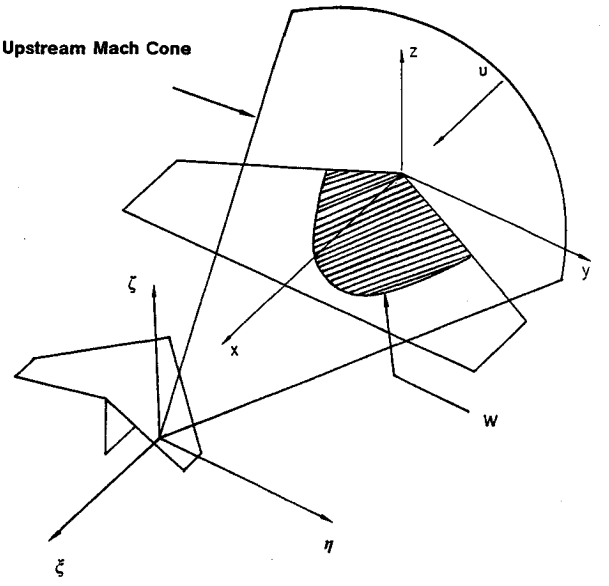

Fig. 1 Coordinate geometry and integration area.

Discretization Procedure

Grid boxes are obtained by using spanwise and chordwise divisions. Two distinct approaches are available for discretizing Eq. (1). The first[15,16] assumes a constant pressure in the jth box, and evaluates the normalwash at the ith control point. The assumption of constant pressure allows ΔC_p to be taken outside the integration sign in Eq. (1), which is carried out over the area of the pressure box intersected by the upstream Mach cone. The other discretization procedure is the doublet-point method,[21] which assumes a concentrated lift force $A_j \Delta C_p$ in each box, whose nondimensional area is A_j, giving the nondimensional pressure difference in the jth box as

$$A_j \Delta C_p(X, Y)\delta(X - X_j)\delta(Y - Y_j)$$

where $\delta(\ )$ is the Dirac delta function. Furthermore, it is assumed that the normalwash in the ith box can be represented by an average value w_i such that

$$w_i = \frac{1}{A_i} \int \int_{\Delta W} w(\xi, \eta)\, d\xi\, d\eta \tag{5}$$

where ΔW is the part of an averaging region lying inside the downstream Mach cone emanating from the load point (X_j, Y_j). The discretized integral equation then becomes

$$w_i = \frac{1}{8\pi} \sum_{j=1}^{N} \frac{A_j}{A_i} \Delta C_{pj} \int \int_{\Delta W} K(x, y, z, \omega)\, dX\, dY \tag{6}$$

Ueda and Dowell[21] selected a rectangular averaging region for the normalwash, with the area and width the same as that of the receiving box, and displaced downstream such that its leading edge passes through the box center (Fig. 2). The load point is assumed to be located at the center of the sending (pressure) box. These choices of the normalwash averaging region and the load point are found to be numerically justified, although no analytical reason is offered for them in Ref. 21. Furthermore, it was found[26] that such averaging regions work when all the boxes are of a uniform width. Trapezoidal averaging regions are also possible,[26] but they increase the number of cases of Mach cone intersection dramatically. All boxes have side edges parallel to the freestream for simplicity.

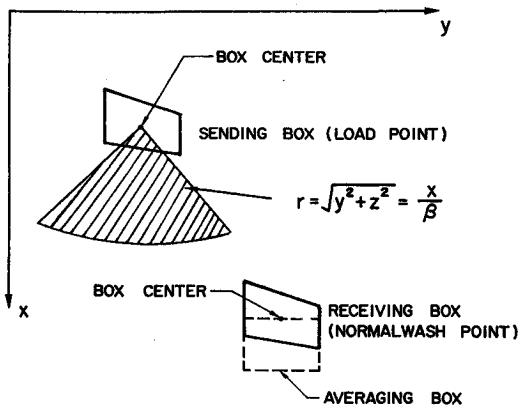

Fig. 2 Discretization and averaging geometry.

Equation (6) requires integration of the kernel function. However, the kernel function has singularities on the Mach cone where $R \to 0$. In order to integrate these strong singularities, the kernel function is simplified to a form given in the Appendix. Since a direct integration of the singular oscillatory kernel is not possible, it is further separated into steady and unsteady factors. The steady factor is obtained by letting $k = 0$, and is expressed as

$$K_s(x, y, z) = \frac{2x}{Rr^2}[T_1 + T_2(\beta^2/R^2 - 2/r^2)] \tag{7}$$

The unsteady factor is obtained by dividing the kernel function by K_s:

$$K_u(x, y, z, k) = \frac{K(x, y, z, k)}{K_s(x, y, z)} \tag{8}$$

The unsteady factor K_u, containing the oscillatory terms, is analytic on the Mach cone, and it can be shown that

$$\lim_{R\to 0} K_u(x, y, z, k) = -[\exp(-ikM^2r/\beta)]/T_2 \tag{9}$$

Since the unsteady factor is varying slowly inside the averaging region, it is evaluated at its center and taken outside the double integral sign. Hence, Eq. (6) becomes

$$w_i = \frac{1}{8\pi}\sum_{j=1}^{N}\frac{A_j}{A_i}\Delta C_p K_u(x_m, y_m, z_m, k)\int\int_{\Delta W} K_s(x, y, z)\,dx\,dy \tag{10}$$

where subscript m refers to the centroid of the rectangular averaging region. As Eq. (10) indicates, only the steady kernel must be integrated. The region of integration ΔW is obtained by the intersection of the Mach cone with the averaging region. The equation describing a Mach cone is $x^2 - \beta^2(y^2 + z^2) = 0$, while an averaging region can be expressed as $z = y\tan(\gamma_r - \gamma_s) + h$, where h is the vertical separation between the sending and receiving points. This gives the equation of the Mach boundary which bounds the region of integration ΔW upstream as

$$y = [-h\tan(\gamma_r - \gamma_s) \pm \sqrt{(x^2/\beta^2)\sec^2(\gamma_r - \gamma_s) - h^2}]\cos^2(\gamma_r - \gamma_s) \tag{11}$$

Figure 3 shows the various possible cases in which the Mach cone can intersect an averaging region.

Kernel Integration

In order to integrate the steady kernel, the integral

$$I = \int_{x_a}^{x_b}\int_{y_a}^{y_b} K_s(x, r)\,dy\,dx$$

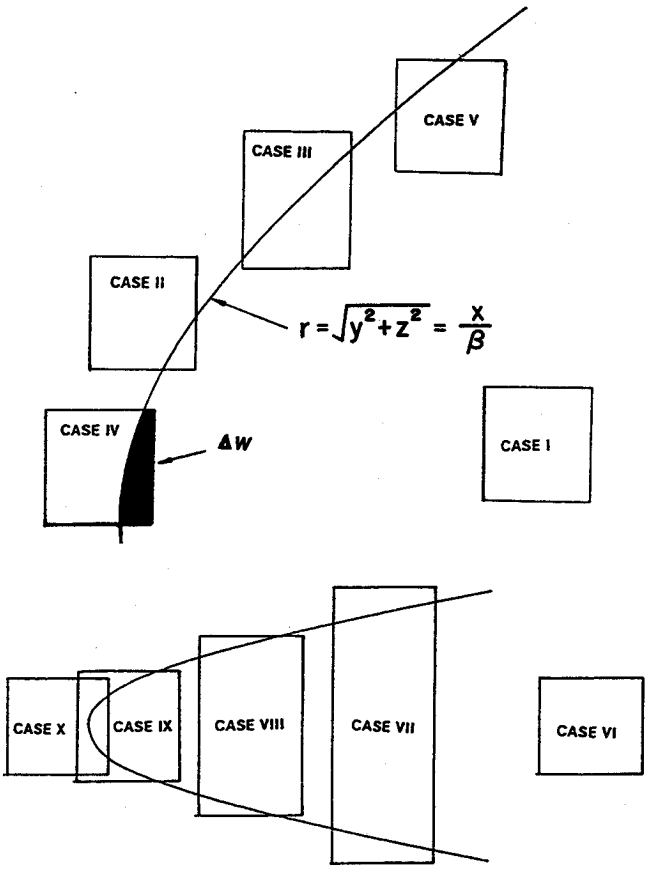

Fig. 3 Averaging cases of Mach cone intersection.

is divided into three parts, $I = I_1 + I_2 + I_3$ where

$$I_1 = T_1\int_{x_a}^{x_b}\int_{y_a}^{y_b}\frac{2x}{Rr^2}\,dy\,dx$$

$$I_2 = -4\int_{x_a}^{x_b}\int_{y_a}^{y_b}\frac{xT_2}{Rr^4}\,dy\,dx$$

$$I_3 = 2\beta^2\int_{x_a}^{x_b}\int_{y_a}^{y_b}\frac{xT_2}{R^3r^2}\,dy\,dx$$

x_a, x_b, y_a, y_b denote the limits of integration corresponding to the area ΔW. The integrals I_1 and I_2 are seen to have a $\frac{1}{2}$ power singularity as $R \to 0$. This singularity is removed by using the relation

$$\frac{\partial R}{\partial x} = \frac{x}{R} \tag{12}$$

When this relation is incorporated into the integrands, the two integrals become

$$I_1 = 2T_1\left[\int_{y_a}^{y_b}\frac{\sqrt{x^2 - \beta^2r^2}}{r^2}\,dy\right]_{x_a}^{x_b}$$

$$I_2 = -4\left[\int_{y_a}^{y_b}T_2\frac{\sqrt{x^2 - \beta^2r^2}}{(y^2 + z^2)^2}\,dy\right]_{x_a}^{x_b}$$

I_1 and I_2 are nonsingular and can be carried out analytically. Integral I_3 contains a $\frac{3}{2}$ power Mach cone singularity, whose treatment requires the consideration of the following integral:

$$\int_{y_a}^{y_b}\frac{\partial}{\partial y_b}\left[\frac{f(y_b, y)}{\sqrt{y_b - y}}\right]dy \tag{13}$$

where

$$f(y_b, y) = (T_2/\beta r^2\sqrt{y_b + y})$$

$$y_b = (1/\beta^2)\sqrt{x^2 - \beta^2 z^2}$$

Since $f(y_b, y)$ is continuous and integrable in the range of integration with the following property:

$$\lim_{y \to y_b} \left[(y_b - y) \frac{\partial}{\partial y_b} f(y_b, y) \right] = 0$$

then Hadamard's[27] "finite part" exists for the integral in expression (13) which is defined as follows:

$$\text{Fp.} \int_{y_a}^{y_b} \frac{\partial}{\partial y_b} \left[\frac{f(y_b, y)}{\sqrt{y_b - y}} \right] dy = \frac{\partial}{\partial y_b} \int_{y_a}^{y_b} \frac{f(y_b, y)}{\sqrt{y_b - y}} dy \quad (14)$$

"Fp." denotes the finite part of the singular integral. The definition of the finite part[27] is such that, instead of taking the integral up to its singular limit where it would diverge, the integrand is expanded in a polynomial series near the point of singularity, and only those terms of the series are retained that remain finite after integration. It is interesting to note that, as shown by Schwartz,[28] Hadamard's finite part for any integral with first-order singularity exactly corresponds to the Cauchy's principal-value for the same integral. Heaslet and Lomax[29] showed that Eq. (14) is also valid for a higher order of differentiation with respect to the integration limit. By substituting the relation

$$\frac{\partial}{\partial y_b} = \beta^2 \frac{y_b}{x} \frac{\partial}{\partial x}$$

in Eq. (14), the following is obtained:

$$\text{Fp.} \int_{y_a}^{y_b} \frac{\partial}{\partial x} \left(\frac{T_2}{Rr^2} \right) dy = \frac{\partial}{\partial x} \int_{y_a}^{y_b} \frac{T_2}{Rr^2} dy \quad (15)$$

The integral on the left side of Eq. (15) is recognized as the inner integral of I_3, whose finite part can now be written as

$$I_3 = -2\beta \left(\int_{y_a}^{y_b} \frac{h^2 \cos(\gamma_r - \gamma_s) + yh \sin(\gamma_r - \gamma_s)\, dy}{\{y^2 + [y \tan(\gamma_r - \gamma_s) + h]^2\}\sqrt{x^2 - \beta^2\{y^2 + [y \tan(\gamma_r - \gamma_s) + h]^2\}}} \right)_{x_a}^{x_b}$$

A half-order singularity remains in the integrand and can be integrated in the sense of Hadamard,[27] to produce

$$I_3 = -\beta \{[g(x, y)]_{y_a}^{y_b}\}_{x_a}^{x_b}$$

where

$$g(x, y) = h \sin(\gamma_r - \gamma_s)\cos^2(\gamma_r - \gamma_s) \sqrt{\frac{\beta}{x}}$$

$$\times \log_e \left\{ \frac{\sqrt{\frac{\beta}{x}} - \sqrt{x^2 - \beta^2\{y^2 + [y \tan(\gamma_r - \gamma_s) + h]^2\}}}{\sqrt{\frac{\beta}{x}} + \sqrt{x^2 - \beta^2\{y^2 + [y \tan(\gamma_r - \gamma_s) + h]^2\}}} \right\}$$

$$- \frac{2h\beta}{x} [\sin^2(\gamma_r - \gamma_s)\cos^2(\gamma_r - \gamma_s) + \cos(\gamma_r - \gamma_s)]$$

$$\times \tan^{-1} \left(\frac{x[h \tan(\gamma_r - \gamma_s) - y \sec^2(\gamma_r - \gamma_s)]}{h\beta\sqrt{x^2 - \beta^2\{y^2 + [y \tan(\gamma_r - \gamma_s) + h]^2\}}} \right)$$

In the coplanar limit ($z = 0$), an r^{-2} singularity of the kernel appears in boxes directly downstream of the sending point, and is integrated in the sense of Mangler,[30] as shown in Ref. 21.

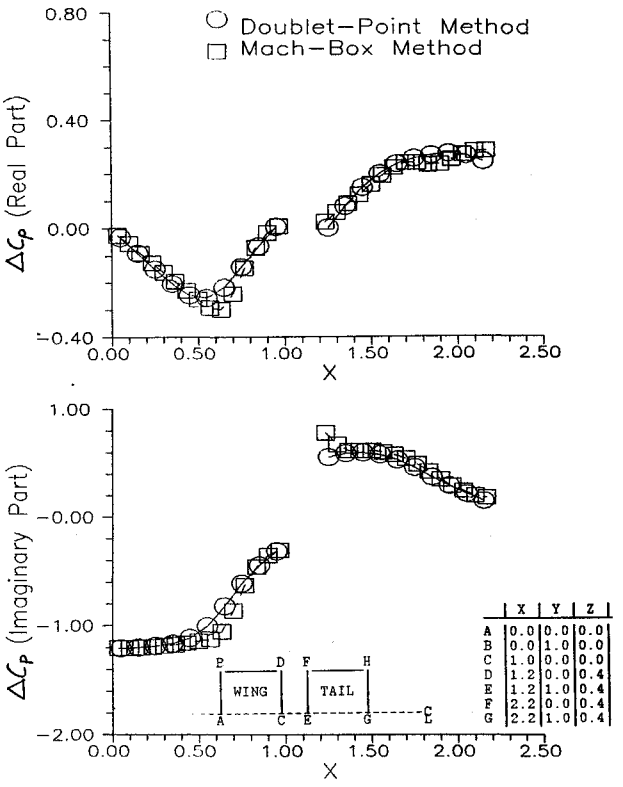

Fig. 4 Chordwise pressure distribution at 5% span for the rectangular wing-tail configuration, wing plunging at $k = 0.2$, $M = 1.2$ (test case I).

Numerical Results

In order to validate the nonplanar doublet-point method, comparisons are presented with other methods for some test cases. The reference length b, used in these test cases for the reduced frequency k, is the semispan of the configurations.

Noncoplanar Rectangular Wing-Tail

This test case examines the nonplanar interference between a rectangular wing and tail, with the tail separated vertically from the wing by 0.4 units. Figures 4–6 show the chordwise pressure distributions at 5, 45, and 95% span locations, respectively, when the wing undergoes uniform plunging oscillations at $k = 0.2$ and $M = 1.2$. Good agreement is observed in these figures with the Mach box method.[7] Results are obtained with 200 boxes in the double-point method (DPM) and 300 boxes on surfaces (plus additional boxes in the diaphragm region) in the Mach box method. References 19 and 20 have also presented results for this case, but at different spanwise locations.

Rectangular Wing with Folded Tips

Here, the nonplanar DPM is applied to a rectangular wing of aspect ratio 4.0, with tip dihedral beginning at the mid-semispan location. The wing is at a steady angle of attack in a stream of $M = \sqrt{2}$. Figure 7 shows the lift-curve slope $C_{L\alpha}$ as a function of the tip dihedral angle γ. Results from Ref. 31 obtained with a Mach box method and an analytical theory[32] are used for comparison. The three results are seen to be in good agreement, although the DPM slightly underpredicts the exact values at high fold angles. Reference 20 also presented results for this test case.

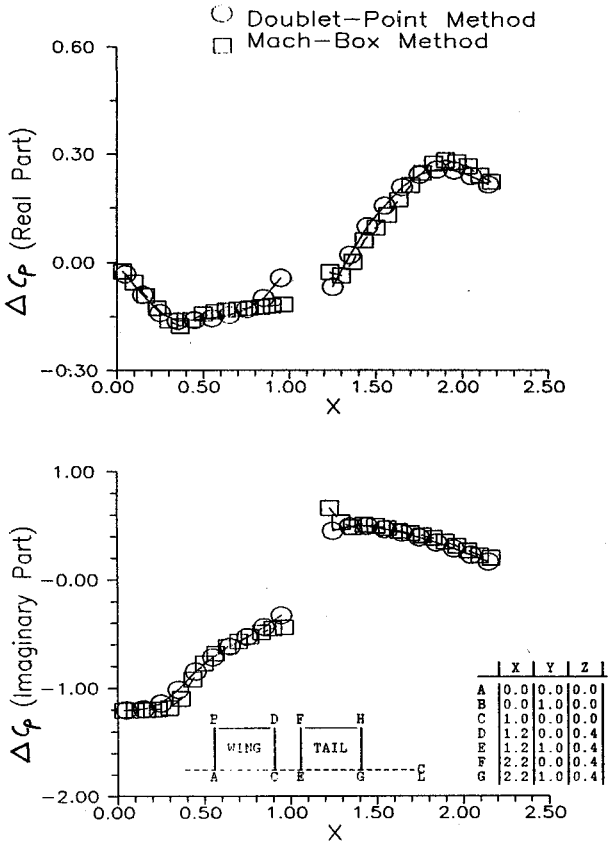

Fig. 5 Chordwise pressure distribution at 45% span for the rectangular wing-tail configuration, wing plunging at $k = 0.2$, $M = 1.2$ (test case I).

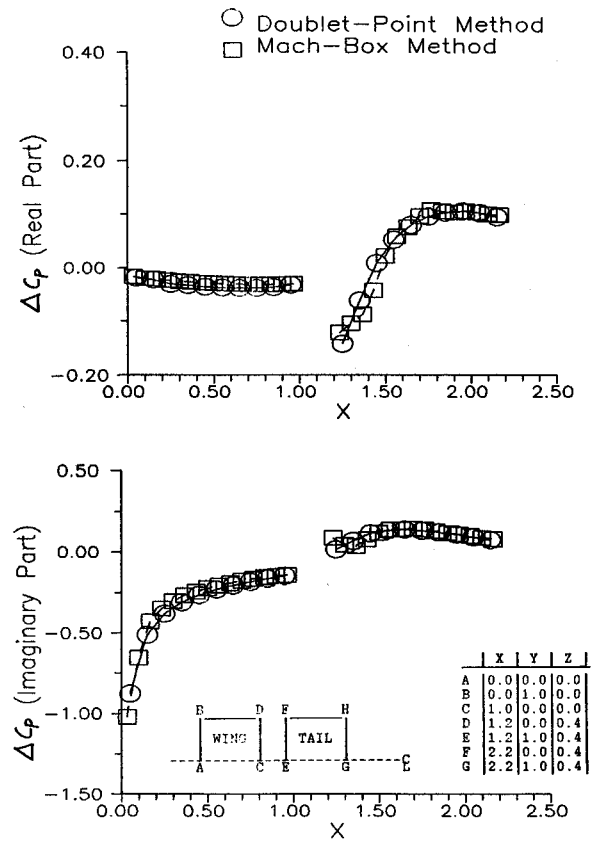

Fig. 6 Chordwise pressure distribution at 95% span for the rectangular wing-tail configuration, wing plunging at $k = 0.2$, $M = 1.2$ (test case I).

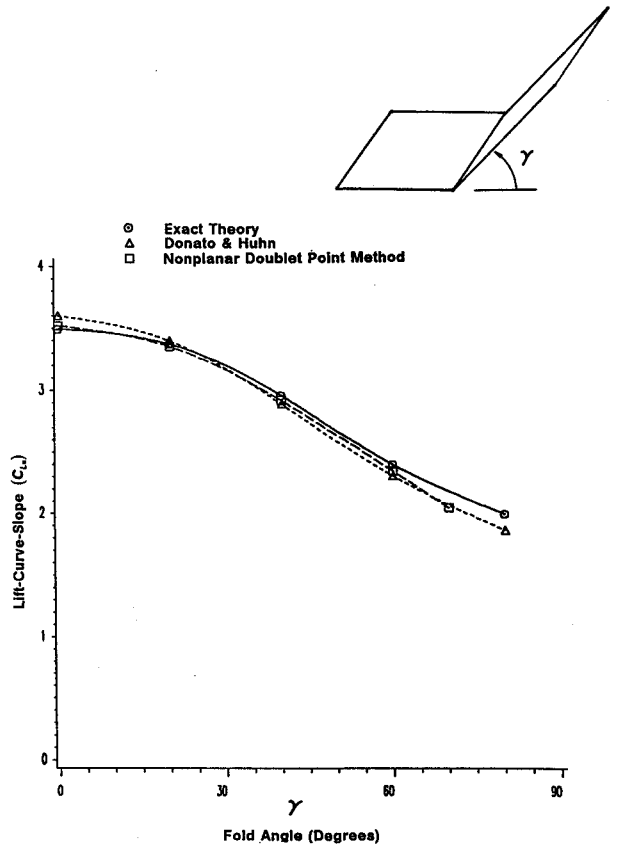

Fig. 7 Variation of lift curve-slope with fold angle for the rectangular wing with folded-tips, $k = 0$, $M = 1.414$ (test case II).

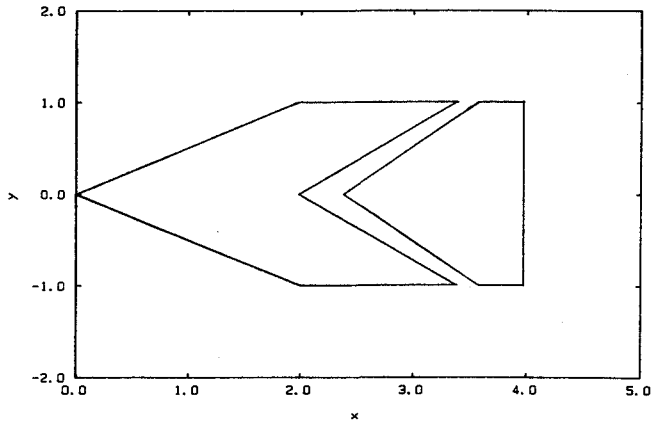

Fig. 8 Noncoplanar swept wing-tail geometry (test case III).

Highly Swept Noncoplanar Wing-Tail

This example tests the applicability of the nonplanar DPM to a highly swept wing-tail interference problem. The planform geometry is shown in Fig. 8, with the tail separated 0.2 units vertically from the wing. The leading-edge sweep angles of the wing and tail are 63.44 and 50.2 deg, respectively. Results from the piecewise continuous kernel function method[20] (PCKFM) are selected for comparison. The PCKFM divides a lifting surface into several boxes whose boundaries are Mach lines. A continuous pressure polynomial is assumed in each box, and control points are collocated for the solution of the polynomial coefficients. In the present example, PCKFM employs 38 unknowns in the pressure polynomial. The chordwise pressure calculations for $M = \sqrt{2}$ and a steady angle of attack are shown in Figs. 9 and 10 for 55 and 80% span locations, respectively. The PCKFM is seen to produce jumps in the pressure distribution, which are not possible in a linearized flow, and are due to the PCKFMs allowing discontinuities in

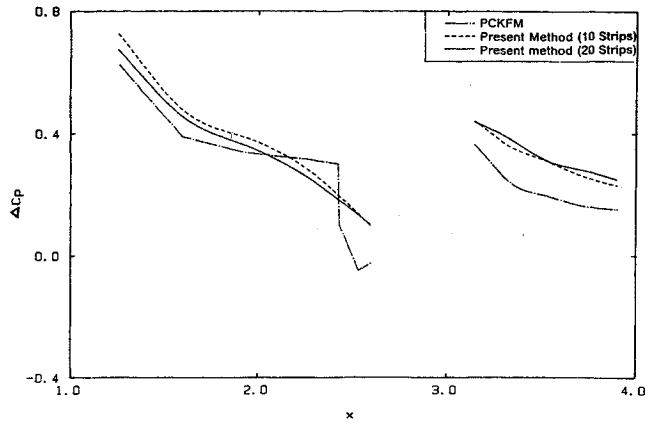

Fig. 9 Chordwise pressure distribution at 55% span for the swept wing-tail configuration at a steady angle of attack, $M = 1.414$ (test case III).

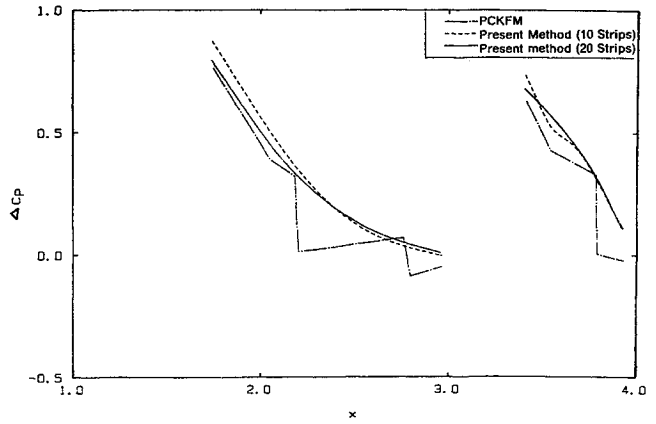

Fig. 10 Chordwise pressure distribution at 80% span for the swept wing-tail configuration at a steady angle of attack, $M = 1.414$ (test case III).

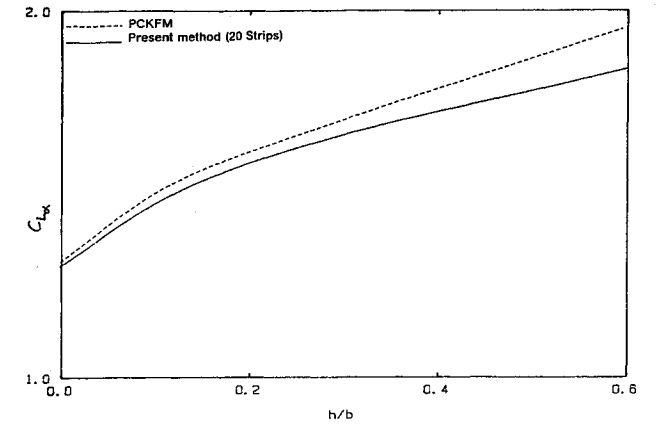

Fig. 11 Variation of the lift curve-slope with vertical separation, $M = 1.414$ (test case III).

the pressure polynomial across Mach lines.[20] In contrast, the DPM results, obtained by taking 10 and 20 spanwise grid divisions (strips), respectively, are seen to be well behaved. In addition, a large disagreement is seen on the tail pressures, which appears to be largely due to an assumption in the PCKFM[20] that the Mach cone boundaries in nonplanar interference can be taken as straight lines, where they are actually hyperbolae.

The variation of the overall $C_{L\alpha}$, with the nondimensional vertical spacing h/b, is presented in Fig. 11. Both PCKFM and DPM show that the steady $C_{L\alpha}$ increases sharply as the vertical spacing assumes a nonzero value. With a further increase in the vertical spacing, the increment in $C_{L\alpha}$ becomes less gradual. The discrepancy between the PCKFM and DPM results is seen to increase with h/b. This is again probably due to the fact that while PCKFM ignores the Mach boundary curvature, which becomes larger with increasing h/b, the DPM accounts for this curvature correctly [Eq. (11)].

F-18 Wing with Leading-Edge Flap

Reference 16 presented results of the recently developed ZONA51C Harmonic-Gradient program for an F-18 wing with oscillating leading-edge flap. Figure 12 shows the planform geometry. The flap is oscillating at $k = 4.0$ in a stream of $M = 1.1$. Chordwise pressure (real part) distribution of Ref. 16 at 58.8% span is compared with that of the DPM in Fig. 13. The figure shows a good agreement between the two methods upon the pressure jump across the hinge-line. However, local fluctuations are observed in the pressure distribution calculated by the DPM near the leading and trailing edges. Since this is a planar case, the cause of such fluctuations does not

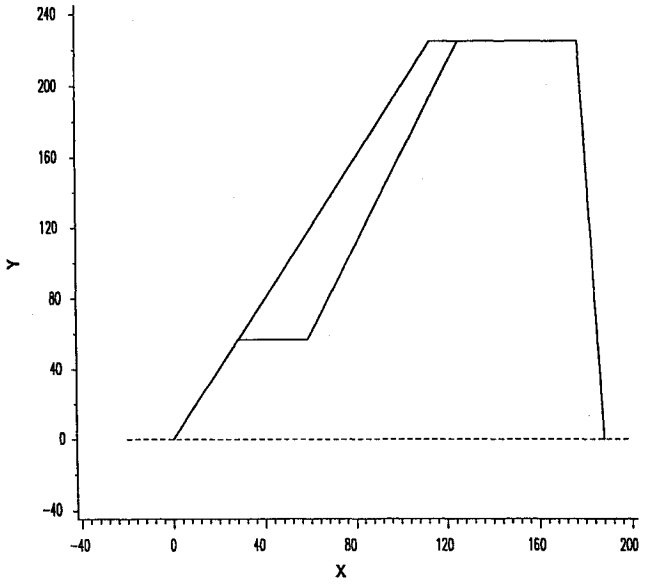

Fig. 12 F-18 wing with a leading-edge flap (test case IV).

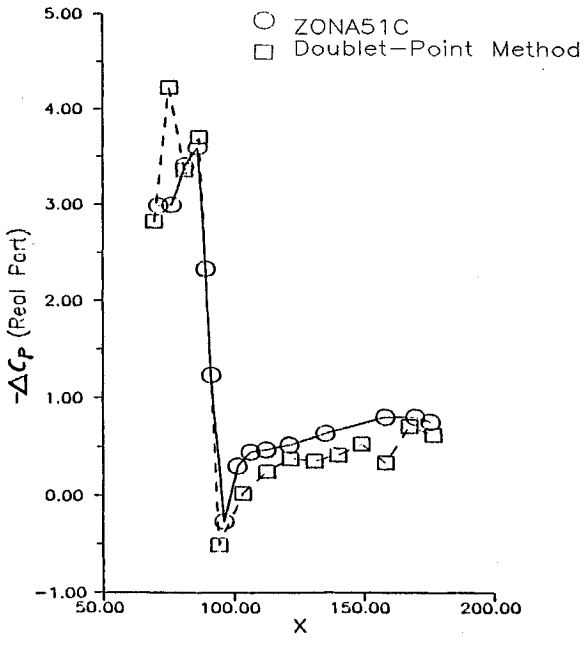

Fig. 13 Chordwise pressure distribution on F-18 wing at 58.8% span, with the leading-edge flap oscillating at $k = 4.0$, $M = 1.1$ (test case IV).

lie in the nonplanar extension presented in this article. Similar chordwise pressure fluctuations were reported by Ueda and Dowell[21] with their planar DPM on swept wings, when boxes of low aspect ratio were used. Although an obvious solution to this problem would seem to be the use of high aspect ratio elements, the spanwise pressure distribution would not be adequately represented by such elements on a surface such as the F-18 wing. Ueda and Dowell[21] attributed the fluctuations to high leading-edge sweep angles, arguing that the DPMs assumption of a concentrated load within a box makes it impossible for a single box to account for the effect of the sweep, since the influence of a box upon itself is always evaluated over a rectangular averaging region (some discussion on the averaging region can be found also in Ref. 33). However, subsequent experiments[26] with the shape of the averaging region revealed that the fluctuations persisted (though occurring at other chordwise locations) when the averaging region was allowed to have the same shape as the receiving box. It appears that the problem is connected to the location of the point doublet within a box, rather than the shape of the averaging region.

The fluctuations in the pressure results of the planar DPM are small in magnitude and do not affect the overall pressure distribution by an appreciable extent. Therefore, they are inconsequential to aeroelastic and flight-dynamic applications, and their presence does not detract from the usefulness of the DPM, considering its advantages in comparison with other schemes. However, the fluctuations point toward the need for an analytical justification for the concept of normalwash averaging, which will lead to a unique shape of the averaging region as well as the final location of the doublet point in a box. The arbitrary choice of these parameters made in Ref. 21 also restricts the DPM to boxes with equal widths.[26] By choosing the correct averaging parameters, this restriction of the supersonic DPM can be removed, thereby making it more general in application.

Conclusions

The concepts of discrete acceleration potential doublets and averaged normalwash are developed into a general nonplanar supersonic doublet point method, without introducing further approximations. The present method offers the greatest degree of commonality with subsonic calculations, and its incorporation into a unified subsonic/supersonic code is the easiest, compared with other possible approaches, differing from the subsonic doublet-point method only in the kernel integration. Although the concept of normalwash averaging is not established analytically, it is seen to be valid for some choices of the averaging region. The scheme can be made more general if an analytical justification can be obtained for the averaging concept, which can lead to a unique selection of the averaging parameters. Special features of the scheme, such as point loads and commonality with the subsonic case, make it attractive for efficient aeroelastic applications on general configurations.

Table A1 Series constants

$c = 0.372$		
n	a_n	b_n
1	−0.24186198	−3.509407
2	2.7968027	57.17120
3	−24.991079	−624.7548
4	111.59196	3830.151
5	−271.43549	−14538.51
6	305.75288	35718.32
7	41.183630	−57824.14
8	−545.98537	61303.92
9	644.78155	−40969.58
10	−328.72755	15660.04
11	64.279511	−2610.093

Appendix

The kernel function given by Eqs. (2–4) can be simplified by using the series expansions of Laschka[34] and Cunningham[19] for the nonrational terms in the integrands, and expressed as

For $X_1 \geq 0$

$$K(x, y, z, k) = e^{-ikx}\left\{T_1\left[\frac{e^{-ikX_1}}{r^2}(x/R + 1) + \frac{e^{-ikX_2}}{r^2}(x/R - 1) - ikA_2/r + ikA_1/r\right] + T_2 e^{-ikX_1}\left[\frac{\beta^2 x}{R^3 r^2} - \frac{2}{r^4}(x/R + 1) - \frac{ikM^3}{R^2(x + X_1)}\right] + T_2 e^{-ikX_2}\left[\frac{\beta^2 x}{R^3 r^2} - \frac{2}{r^4}(x/R - 1) + \frac{ikM^3}{R^2(x + X_2)}\right] + T_2(3ikA_2/r^3 - 3ikA_1/r^3 - ikB_2/r^3 + ikB_1/r^3)\right\}$$

For $X_1 < 0$

$$K(x, y, z, k) = e^{-ikx}\left\{T_1\left[(x/R - 1)\left(\frac{e^{-ikX_1}}{r^2} + \frac{e^{-ikX_2}}{r^2}\right) + 2/r^2 + ikA_3/r - ikA_2/r + 2k^2A_4\right] + T_2 e^{-ikX_1}\left[\frac{\beta^2 x}{R^3 r^2} - \frac{2}{r^4}(x/R - 1) - \frac{ikM^3}{R^2(x + X_1)}\right] + T_2 e^{-ikX_2}\left[\frac{\beta^2 x}{R^3 r^2} - \frac{2}{r^4}(x/R - 1) + \frac{ikM^3}{R^2(x + X_2)}\right] + T_2(-4/r^4 - 6k^2A_4/r^2 - 3ikA_3/r^3 + 3ikA_2/r^3 + 2k^2B_4/r^2 - ikB_2/r^3 + ikB_3/r^3)\right\}$$

where

$$A_1 = \sum_{n=1}^{11} \frac{a_n \exp[-(nc + ikr)X_1/r]}{nc + ikr}$$

$$A_2 = \sum_{n=1}^{11} \frac{a_n \exp[-(nc + ikr)X_2/r]}{nc + ikr}$$

$$A_3 = \sum_{n=1}^{11} \frac{a_n \exp[(nc - ikr)X_1/r]}{nc - ikr}$$

$$A_4 = \sum_{n=1}^{11} \frac{a_n}{(nc)^2 + (kr)^2}$$

$$B_1 = \sum_{n=1}^{11} \frac{b_n \exp[-(2nc + ikr)X_1/r]}{2nc + ikr}$$

$$B_2 = \sum_{n=1}^{11} \frac{b_n \exp[-(2nc + ikr)X_2/r]}{2nc + ikr}$$

$$B_3 = \sum_{n=1}^{11} \frac{b_n \exp[(2nc - ikr)X_1/r]}{2nc - ikr}$$

$$B_4 = \sum_{n=1}^{11} \frac{b_n}{(2nc)^2 + (kr)^2}$$

The coefficients c, a_n, and b_n are given in Table A1.

Acknowledgments

Part of this work was carried out at the University of Missouri—Rolla, Rolla, Missouri, supported by a Research Grant from McDonnell Aircraft Company, St. Louis, Missouri.

References

[1]Albano, E., and Rodden, W. P., "A Doublet Lattice Method for Calculating Lift Distributions on Oscillating Lifting Surfaces in Subsonic Flows," *AIAA Journal*, Vol. 7, No. 2, 1969, pp. 279–285.

[2]Giesing, J. P., and Kalman, T. P., "Oscillating Supersonic Lifting Surface Theory Using a Finite Element Doublet Representation," AIAA Paper 75-761, May 1975.

[3]Garrick, I. E., and Rubinow, S. I., "Theoretical Study of Airforces on an Oscillating or Steady Thin Wing in a Supersonic Flow," NACA Rept. 872, 1947.

[4]Pines, S., Dugundji, J., and Neuringer, J., "Aerodynamic Flutter Derivatives for a Flexible Wing with Supersonic and Subsonic Edges," *Journal of the Aeronautical Sciences*, Vol. 22, Oct. 1955, pp. 693–700.

[5]Stark, V. J. E., "Calculation of Aerodynamic Forces on Two Oscillating Finite Wings at Low Supersonic Mach Numbers," SAAB T.N. 53, Linköping, Sweden, 1964.

[6]Fenain, M., and Guiraud-Vallee, D., "Calcul Numerique des Ailes en Regime Supersonique Stationnaire ou Instationnaire," La Recherche Aerospatiale, No. 115, 1966, No. 116, 1967.

[7]Ii, J. M., Borland, C. J., and Hogley, J. R., "Prediction of Unsteady Aerodynamic Loadings of Nonplanar Wings and Wing-Tail Configurations in Supersonic Flow," Pt. 1, Air Force Flight Dynamics Lab., AFFDL-TR-71-108, Pt. 1, March 1972.

[8]Chipman, R. R., "An Improved Mach-Box Approach for Supersonic Oscillatory Pressures," *Journal of Aircraft*, Vol. 14, No. 5, 1977, pp. 887–893.

[9]Ii, J. M., "Refined Prediction Method for Supersonic Nonsteady Aerodynamics with AIC Partition Scheme," *Journal of Aircraft*, Vol. 18, No. 8, 1981, pp. 609–617.

[10]Evvard, J., "Use of Source Distribution for Evaluating Theoretical Aerodynamics of Thin Finite Wings at Supersonic Speeds," NASA TR-951, June 1949.

[11]Burkhart, T. H., "Numerical Application of Evvard's Supersonic Wing Theory to Flutter Analysis," AIAA Paper 80-0741, May 1980.

[12]Jones, W. P., and Appa, K., "Unsteady Supersonic Aerodynamic Theory for Interfering Surfaces by the Method of Potential Gradient," NASA CR-2898, Oct. 1977.

[13]Hounjet, M. H. L., "An Improved Potential Gradient Method to Calculate Airloads on Oscillating Supersonic Interfering Surfaces," *Journal of Aircraft*, Vol. 19, No. 3, 1982, pp. 390–399.

[14]Chen, P. C., and Liu, D. D., "A Harmonic Gradient Method for Unsteady Supersonic Flow Calculations," *Journal of Aircraft*, Vol. 22, No. 3, 1985, pp. 371–379.

[15]Appa, K., "Constant Pressure Panel Method for Supersonic Unsteady Airload Analysis," *Journal of Aircraft*, Vol. 24, No. 5, 1987, pp. 696–702.

[16]Liu, D. D., et al., "Further Studies of the Harmonic Gradient Method for Supersonic Aeroelastic Applications," *Journal of Aircraft*, Vol. 28, No. 5, 1991, pp. 598–605.

[17]Watkins, C. E., and Berman, J. H., "On the Kernel Function of the Integral Equation Relating Lift and Downwash Distributions of Oscillating Wings in Supersonic Flow," NACA Rept. 1257, 1956.

[18]Harder, R. L., and Rodden, W. P., "Kernel Function for Nonplanar Oscillating Surfaces in Supersonic Flow," *Journal of Aircraft*, Vol. 8, No. 4, 1971, pp. 677–679.

[19]Cunningham, A. M., Jr., "Oscillatory Supersonic Kernel Function Method for Interfering Surfaces," *Journal of Aircraft*, Vol. 11, No. 6, 1974, pp. 664–670.

[20]Lottati, I., and Nissim, E., "Nonplanar, Supersonic Three-Dimensional, Oscillatory, Piecewise Continuous Kernel Function Method," *Journal of Aircraft*, Vol. 24, No. 1, 1987, pp. 45–54.

[21]Ueda, T., and Dowell, E. H., "Doublet-Point Method for Supersonic Unsteady Lifting Surfaces," *AIAA Journal*, Vol. 22, No. 2, 1984, pp. 179–186.

[22]Ueda, T., and Dowell, E. H., "A New Solution Method for Lifting Surfaces in Subsonic Flow," *AIAA Journal*, Vol. 20, No. 3, 1982, pp. 348–355.

[23]Rodden, W. P., "Comment on 'A New Solution Method for Lifting Surfaces in Subsonic Flow'," *AIAA Journal*, Vol. 22, No. 1, 1984, p. 160.

[24]Ueda, T., and Dowell, E. H., Reply by the Authors to the Comment on "A New Solution Method for Lifting Surfaces in Subsonic Flow," *AIAA Journal*, Vol. 22, No. 4, 1984, pp. 575, 576.

[25]Tewari, A., "Nonplanar Doublet-Point Method in Supersonic, Three Dimensional, Unsteady Aerodynamics," M.S. Thesis, Univ. of Missouri—Rolla, Rolla, MO, 1988.

[26]Tewari, A., "New Acceleration Potential Method for Supersonic Unsteady Aerodynamics of Lifting Surfaces, Further Extension of the Nonplanar Doublet Point Method, and Nonlinear, Nongradient Optimized Rational Function Approx. for Supersonic, Transient Response Unsteady Aerodynamics," Ph.D. Dissertation, Univ. of Missouri—Rolla, Rolla, MO, 1992.

[27]Hadamard, J., "Lectures on Cauchy's Problem in Linear Partial Differential Equations," Yale Univ. Press, New Haven, CT, 1928.

[28]Schwartz, L., "Theorie des Distributions," Nouvelle ed., Hermann, Paris, 1966.

[29]Heaslet, M. A., and Lomax, H., "Supersonic and Transonic Small Perturbation Theory," Chap. 3, General Theory of High Speed Aerodynamics, Princeton Univ. Press, Princeton, NJ, 1954.

[30]Mangler, K. W., "Improper Integrals in Theoretical Aerodynamics," Royal Aircraft Establishment, RAE Rept. Aero. 2424, 1951.

[31]Donato, V. W., and Huhn, C. R., Jr., "Supersonic Unsteady Aerodynamics for Wings with Trailing Edge Control Surfaces and Folded Tips," Air Force Flight Dynamics Lab., AFFDL-TR-68-30, Aug. 1968.

[32]Rodemich, E. R., "Analytical Solution of an Interference Problem in Supersonic Flow," North American Aviation, Rept. SID 65-695, June 1965.

[33]Ueda, T., and Dowell, E. H., Reply by the Authors to the Comment on "Doublet-Point Method for Supersonic Unsteady Lifting Surfaces," *AIAA Journal*, Vol. 23, No. 6, 1985, pp. 979, 980.

[34]Laschka, B., "Zur Theorie der harmonisch Schwingenden tragenden Flache bei Unterschallanstromung," Zeitschrift Fur Flugwissenshaften, 11 Jahrgung, Heft 7, Juli 1963.